ENHANCED REGIONAL NUMERICAL PREDICTION SYSTEM AND ITS PERFORMANCE

Yan Jinghua (阎敬华), Wang Zaizhi (王在志) and Xue Jishan (薛纪善)

Guangzhou Institute of Tropical and Oceanic Meteorology, Guangzhou 510080

Received 14 November 1995, accepted 19 March 1996

ABSTRACT

During the "8th Five-Year Plan" (1991~1995), a new operational mesoscale numerical prediction system is developed, which is called the "Regional Enhanced Numerical Prediction System". The system possesses higher resolution (45 km grid size in horizontal, 10 layers in vertical), as well as full physical processes, and can be run operationally in the Guangzhou Regional Meteorological Centre (GRMC). A plenty of experiments indicate its better performance in predicting various weather systems affecting the south of China, especially the typhoon and heavy rain in the "early floods stage" (annually speaking). Verification of the prediction of all typhoon cases affecting the region in 1993~1995 indicate that rainfall prediction scores of the system are obviously higher than those of the LAFS in the National Meteorological Centre, and track prediction error is no larger than those of NWPs in main world centres such as the National Hurricane Center of NOAA and the JMA. The aim of the paper is to give a generalized introduction and analysis to the system and its performance.

Key words: enhanced numerical prediction, experiment of prediction, performance

I. INTRODUCTION

Numerical weather prediction and its applications have been rapid worldwide over the past few decades. Global and regional model systems of assimilation, analysis, and prediction have been successively developed in the European Center for Medium-range Weather Forecast (ECMWF), United States and Canada and a number of nations and centers. Over the previous few years, the tendency has been towards the increase of resolution and development of meso-and fine-scale forecast systems. Meso-scale routine model systems have been set up in Britain, U. S. A., Japan, Canada, France, Germany and Denmark (Chen and Yan, 1995). At present, the resolution is 30 km in such models in America and Japan while it is 15 km in Britain, which is fine enough for detailed analysis and forecast of various synoptic regimes and mesoscale phenomena. With respect to models for forecasting tropical cyclones, there are special (or general) models of 40-110 km resolution in Japan, America, Britain, Australia and ECMWF (Chen, 1995), showing a general tendency towards mesoscale. Similar efforts are being made in China in that five-day medium-range (Model T42L9) and seven-day global (Model T63L16) numerical predictions were operationally available in 1992 and 1994, respectively, marking a milestone in her development of numerical analysis, assimilation, and prediction system towards advanced world level. The resolution is being improved. On the other hand, numerical forecasting for tropical cyclones and hard rain has been confined to large-scale models that only included simple physical processes due to conditional restraints. It is, however, uncomfortably true that the hard rain associated with the tropical cyclone is closely linked with meso-and fine-scale condition, and it calls for development of mesoscale model prediction systems that both reflect the effects of mesoscale regimes and take account of various roles of physical processes, for the purpose of refining model

resolution. Special treatment is needed in the aspects of data assimilation and model physics as low-latitudes has been where the difficulty and shortcomings are predominant in numerical prediction. A general introduction to a newly-developed regional enhanced numerical prediction system (shortened as ENPS) is made in this paper.

Ⅱ. INTRODUCTION TO ENPS

The system (ENPS) is made up of analysis and assimilation, dynamic modeling and post-processing of NWP, which are so connected that a complete system that runs in a fully automatic manner in operation is formed. Fig. 1 is a diagram of operational ENPS flow. Incessantly through the system, two 48-h forecasts are output daily at 1200 and 0000 GMT, in which the operation of assimilation and analysis, and model forecast are performed on DEC/AXP3800 having a command speed of 500 MIPS and that of graphic drawing and output on VAX6420. It takes only a little more than fifty minutes for the whole system to operate from start-up to provision of 48-h forecast products, meeting the needs of routine operations concerning the validity of time. A brief account is given of each individual components of ENPS.

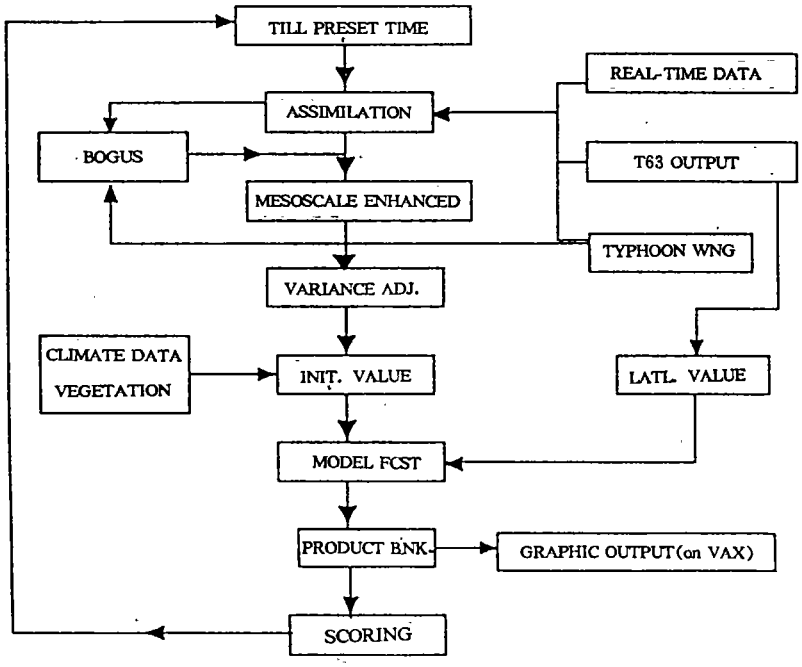

Fig. 1 Operational flow diagram for the ENPS.

1. *Assimilation and analysis*

The procedure is executed in three steps. Step one, objective analysis is done of the observations using multivariate four-dimensional optimum interpolation scheme. Wind-pressure relation and divergent winds are treated to adapt to the special conditions of atmospheric motion in low-latitudes. The first guess is the analysis (for 1200 GMT) or 12-h forecasts (for 0000 GMT) by T63 global model predictive system, Beijing. As the T63

is a global assimilation and predictive system at 6-h intervals, a relatively reasonable and coordinated field of analysis and forecast is available even for the tropical ocean that suffers from insufficient data observed, being one of the causes behind the use of T63 product as the first guess for regional analysis. On the other hand, the choice is attributable to highest possible exploitation of information analyzed and forecast by global models of the national center in high-resolution regional predictive systems, which is required by consistent development in the overall plan of numerical weather prediction in China. It is also the reality in America, Canada, and Japan. In the scheme, not only various sources of information (radiosounding, anemological measurement, T63, ECMWF, KWBC, surface and ship reports, airplane and satellite surveillances) are fully used to recover as much weather signals as possible, but coordination and consistency are attained among different variates to facilitate the model forecast. A univariate analysis scheme is incorporated for relative humidity in view of the parcularity of the moisture field (see separate paper for details)①.

In Step 2, when a tropical cyclone appears, the above-mentioned assimilated field and typhoon warnings are used to construct a conceptual typhoon bogus that satisfies gradient-wind, static, and quasi-thermal equilibria, and gets coordinated with parameterized convection and includes the secondary circulation and initial motion of the storm as well. The bogus is embedded into the analysis field once or twice. It is now widely accepted that one of the effectice ways to improve the accuracy of prediction of typhoons, mostly active on tropical oceans, is setting up a bogus storm, in the face of insufficient observation (Chen, 1995). General guidelines to the application of the scheme is referred to He and Wang (1993).

More analysis, now on the mesoscale, is needed, as in Step 3, to supplement the results obtained in the two steps above, though they are giving good forecast as shown in many model experiments. ENPS is a mesoscale system that copes with phenomena at relatively finer scale from dozens of to hundreds of km, against the environment that the optimum interpolation scheme is capable of using data with all levels of error and different variates in coordination while showing too coarse a resolution in depicting the meso- and small-scale distribution of the variates. It is, therefore, necessary to further modify the field with the Cressman's successive correction scheme for better reflection of mesoscale signature of the observing station. The added analysis, carried out entirely on horizontal model grids of 45-km resolution, avoids possible errors of values horizontally interpolated at a coming step. Tests have shown a substantial increase of analysis and forecast of mesoscale weather phenomena.

2. *Formation of initial and lateral values*

Reflecting more mesoscale information, the successively corrected results are inevitably accompanied by inconsistency among the variates. Variational adjustment (or, weak constraining) is performed that includes wind-pressure equilibrium, and advective and frictional effects. It is shown in tests that the wind-pressure field is much more coordinated with variational modification, the concrete steps being referred to Xue and Wang (1992).

Surface elements are also analyzed. To solve the inconsistency between the model

① Wang Zaizhi, Yan Jinghua and He Xicheng, 1996. Regional enhanced system of assimilation and analysis, *Journal of Tropical Meteorology* (Chinese edition, in press).

and real topography, mandatory surface pressure related to topography is introduced to interpolate meteorological elements observed (in the form of deviation from the standard for the pressure) onto the model grids for variational adjustment. The pressure deviations so adjusted are superimposed into the standard to form model surface pressure, thus avoiding errors of initial surface pressure brought forth by interpolation of geopotential values at the level of ground surface.

After the variational adjustment, the variate is vertically interpolated to the σ-plane to initialize the model atmosphere. Specifically, the earth and subsurface temperature, vegetation and albedo are determined with reference to the climatological mean and output of T63 and the topographic height is available from the mean height field in area of 0.5°×0.5°. The initialization scheme, employed in ENPS for non-linear normalization of the model, proves to be effective in dealing with the noise intrinsically with the initial model atmosphere. The lateral conditions are highly essential for mesoscale models covering a limited area. Sound lateral conditions, being realistic and consistent at least, are a must for the model to be effective for up to 48 h. It is thus necessary that the lateral conditions for ENPS are provided by a larger-scale model until the T63 output gets operationally useful. The former' s lateral values are now an alternative.

3. *The numerical model*

The mesoscale research model by PENN STATE/NCAR (MM4) being the basic frame, the numerical model in question has been updated and operational. Taking hydrostatic equilibrium state by σ-coordinated flux-type primitive equations, the model is mainly governed by

$$\frac{\partial P^* u}{\partial t} = -m^2\left(\frac{\partial P^* uu/m}{\partial x} + \frac{\partial P^* vu/m}{\partial y}\right) - \frac{\partial P^* u\dot{\sigma}}{\partial \sigma} - mp^*\left[\frac{RT_v}{P^* + P_t/\sigma}\right]\frac{\partial P^*}{\partial x} + \frac{\partial \phi}{\partial x}\Big] + fP^* v + F_H u + F_v u \quad (1)$$

$$\frac{\partial P^* v}{\partial t} = -m^2\left(\frac{\partial P^* uv/m}{\partial x} + \frac{\partial P^* vv/m}{\partial y}\right) - \frac{\partial P^* v\dot{\sigma}}{\partial \sigma} - mp^*\left[\frac{RT_v}{(P^* + P_t/\sigma)}\right]\frac{\partial P^*}{\partial y} + \frac{\partial \phi}{\partial y}\Big] + fP^* u + F_H v + F_v v \quad (2)$$

$$\frac{\partial P^*}{\partial t} = -m^2\left(\frac{\partial P^* u/m}{\partial x} + \frac{\partial P^* v/m}{\partial y}\right) - \frac{\partial P^* \dot{\sigma}}{\partial \sigma} \quad (3)$$

$$\frac{\partial P^* T}{\partial t} = -m^2\left(\frac{\partial P^* uT/m}{\partial x} + \frac{\partial P^* vT/m}{\partial y}\right) - \frac{\partial P^* T\dot{\sigma}}{\partial \sigma} + \frac{RT_v\omega}{C_{Pm}(\sigma + P_t/P^*)} + \frac{P^* Q}{C_{Pm}} + F_H T + F_v T \quad (4)$$

$$\frac{\partial \phi}{\partial \ln(\sigma + p_t/p^*)} = -RT_v \quad (5)$$

$$\frac{\partial P^* q_v}{\partial t} = -m^2\left(\frac{\partial P^* uq_v/m}{\partial x} + \frac{\partial P^* vq_v/m}{\partial y}\right) - \frac{\partial P^* q_v\dot{\sigma}}{\partial \sigma} + P^* P_{CON} + F_H q_v + F_v q_v \quad (6)$$

where the symbols are what they stand for in the usual sense for consideration of complete inclusion of physical processes in the model. The set of equations is coordinated on the Lambert's conformal projection map with 15°N and 30°N as the normal latitudes.

Variates distributing in the Arakawa B leap -frog format, the model has a total of 55×55 horizontal grids (for measuring the wind), at the interval of 45 km (on the surface map) and is topped at 100 hPa. The information about the initial position and motion of the tropical cyclone is dynamically taken from relevant warnings for automatic determination of the center of the model domain around which the storm is made to stay as continnally as possible. When two or more typhoons are active at once, the one that is most likely to have influence on the south of China is isolated by the system to adjust the model condition to it. When it is free from tropical cyclone activity, the model domain becomes square that is sided in about 2400×2400 km and centered at Guangzhou and retains mesoscale topographic distribution (figure omitted). For the integration over time, the central differencing is used together with the time-smoothing scheme for pressure gradient (Brown and Campana, 1978) so that the time step is made much longer. Concurrently, each of the variates is high-frequency filtered to reduce pile-up of corresponding energy. The model incorporates physical processes of quadrivalent horizontal diffusion of eddies on the quasi-p plane (Yan and Xue, 1995), bulk dynamic planetary boundary layer, super-mixing -layer vertical diffusion in the K theory, saturation condensation at resolvable scale, cumulus convection effects containing eddy transportation, dry convection adjustment for maintenance of stability, and predictive scheme of earth temperature by "thin-layered" forced recovery, in which cloudage and diurnal variation is included in solar radiation that is computed with time-efficient table. The time step is 90 s.

The guidelines for selecting the scheme of embedding lateral boundary follows Yan (1987) and it is decided upon by an experiment shown below. First of all, a number of widely-used schemes are tested for comparison, such as the sponge, radiative, fixed and relaxed types, for a final optimum scheme. As is suggested in the experiment, the sponge scheme is relatively better than the rest by reproducing effects close to "realistic" boundary scheme (figure omitted). In contrast, computation is sometimes unstable with the ralaxed scheme. For the selected scheme, we have

$$\left(\frac{\partial F}{\partial t}\right)_n = W(n)\left(\frac{\partial F}{\partial t}\right)_{MS} + (1 - W(n))\left(\frac{\partial F}{\partial t}\right)_{LS} \tag{7}$$

where

$$n = \begin{cases} 1,2,3,4 & \text{variate with respect to nodal point} \\ 1,2,3,4,5 & \text{variate with respect to cyclic point} \end{cases}$$

and F can be any variate, the subscript MS is the tendency of forecast in ENPS and LS the one in the large model; n is the number of grid points (circles) calculated from the lateral boundary towards the inner domain, the most outward circle being weighted at $w(1) = 0$, e. g. the tendency is fully dependent of the large model, while the inner model domain is weighted at $w(n) = 1$ (being larger than 5 and 4 respectively with respect to the circlic and nodal points), e. g. the tendency is totally variable with ENPS itself; the value of $w(n)$ is transitive between them by a given form of function (see Perkey and Kreisberg, 1976). The difference takes the form of

$$\left(\frac{\partial F}{\partial t}\right)_{LS} = (F_{t+\Delta t} - F_t)/\Delta t \tag{8}$$

where F_t and $F_{t+\Delta t}$ stand for the forecasts at time t and $t+\Delta$ by the large model. When

nested with T63 and at the moment of $\Delta t=12$ h, the value taken for F is the one shown on the σ-plane in ENPS with the analysis of T63 on the P-plane (accomplished by reinitialization at individual time). When the nesting is done, however, with the limited-area model (on the σ-coordinates), extra experiments are carried out to filter out the noise accompanied with prediction by the larger-scale model, due to the fact that the time series in such models is usually concurrent with noise fluctuation that is so large that it is affecting the determination of forecasting tendency for a given period. The basic idea follows that the value taken for a predictant $F^*(t)$ in a larger model as lateral boundary condition at, say, a forecast time t (corresponding to the time step n), is treated with high-frequency filtering at some extent, i.e. by

$$F^*(t) = \sum_{k=-\Delta n}^{\Delta n} q(k) \times F(n-k) \tag{9}$$

where $q(n)$ is responding function (weight) and Δn is the time step for integration in response to Δt. As shown in the study, good filtering results are produced with $\Delta t=3$—6 h and $\Delta t=3$ h is selected here. It is worth noting that the procedure covered by Eq. (9) is performed as part of the integration in the larger model, thus sharing no extra hardware resources of CPU. For $q(n)$, two schemes are tested for a value selected as in

$$(1)\quad q(n) = \frac{1}{2\Delta n + 1} \tag{10}$$

$$(2)\quad q(n) = \left\{\frac{\sin[n\pi/(\Delta n+1)]}{(11)\ n\pi/(\Delta n+1)}\right\}\left[\frac{\sin(n\theta_c)}{n\pi}\right] \tag{11}$$

where Eq. (11) is the high-frequency filtering function used in digital filter initialization (see Lynch, 1992). For clear denotation, the filter scheme in Eq. (10) is referred to as a smoothing scheme and the one in Eq. (11) as a weighting scheme.

An ENPS forecast experiment with the motion of a severe tropical cyclone in 1994 (Russ) is carried out using the spongy nesting scheme with different procedures of filtering and updating periods for boundary tendency Δt (figure omitted) and shows that in schemes of unfiltered, smoothed, weighted and fixed boundary at $\Delta t=6$ h and $\Delta t=12$ h, respectively, the weighting scheme with $\Delta t=6$ h yields the best result of all, followed by the smoothing scheme with the same period of boundary updating. The former scheme is selected.

Then, to reduce error induced from interpolation, grid point forecast values in the larger model is directly interpolated onto ENPS instead of a previous, identical process for the mandatory surfaces, in the sequence of

(1) horizontal interpolation of larger model's values from the surface to horizontal grids in ENPS ($F_L \rightarrow F_M$);

(2) computation of difference in topographic altitude on ENPS grids between the two models (Δh);

(3) derivation of surface pressure for the small model based on surface pressure interpolated from the grids of the large model through correction of Δh;

(4) computation of pressure on all surfaces in the small model based on its ground values;

(5) vertical interpolation of the large model's value F_M onto surfaces ($F_M \rightarrow F_{LS}$) in the small model; and

(6) derivation of the large model's tendency ($\Delta F_{LS}/\Delta t$) on grids of the small one based on the difference between two consecutive time.

4. *Products and scores*

Products by this system include high-resolution analysis and forecast fields of all major meteorological elements, with the emphasis on rainfall, motion and high winds associated with the tropical cyclone. Specifically, the predicted results of ground surface winds are available by means of derivation of equation sets governing surface motion that include effects of fine-scale topographic features, on basis of the model forecast through variational method.

Scores are mainly evaluated with regard to rainfall, surface winds and motion of the tropical cyclone. Elements like the wind, pressure, and temperature are not specially scored due to limitation of the model size from the CBS standard. The TS (Threat Score) is adopted. A total of 41 networked observation stations of rainfall in the south of China are selected for verification (Fig. 2). For each of the stations, four model grids are located in the most vicinity of it. If a certain level of rainfall is forecast by one of the

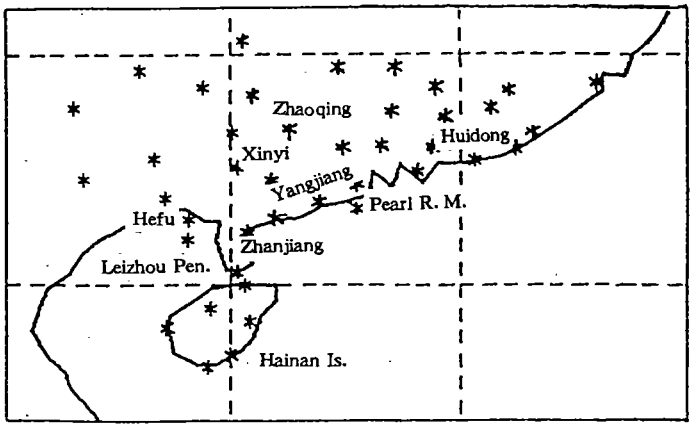

Fig. 2. Stations selected for Treate-score.

grids, it is creditable to this particular station; if rainfall on the same scale is also observed at it, then the forecast is labeled a hit, or a false otherwise. Five levels of 24-h cumulative rainfall are divided for both the predicted and observed amount, with the critical values setting at 1, 10, 25, 50, and 100 mm. A level of rainfall will not be validated unless it is greater than or equal to a certain criterion. There could be four cases of possibility as regard to whether a forecast for a particular level of rainfall is correct or not (Table. 1). In the table, Na is the number of stations for which rainfall is correctly forecast, Nb and Nc are the cases for which rainfall is falsely forecast or missed, and Nd is the number of stations for which lack of rainfall is correctly forecast. Verification of rainfall at all levels is computed using the formula followed.

Table 1. Classification of precipitation forecast.

	With FC	Without FC
With obsv	Na	Nc
Without obsv	Nb	Nd

$$TS = \frac{Na}{Na + Nb + Nc} \quad \text{(TS Scoring)} \quad (12)$$

$$B = \frac{Na + Nb}{Na + Nc} \quad \text{(Deviation)} \quad (13)$$

$$Po = \frac{Nc}{Na + Nc} \quad \text{(Rate of miss)} \quad (14)$$

$$Nh = \frac{Nb}{Na + Nb} \quad \text{(Rate of false)} \quad (15)$$

$$Eh = \frac{Na + Nd}{Na + Nb + Nc + Nd} \quad \text{(Forecast efficiency)} \quad (16)$$

Generally, the larger TS and Eh (unity at the utmost), the closer B is to unity, and the smaller Po and Nh, the better. They are to be analyzed comprehensively to reflect the true level of rainfall forecast.

Ⅲ. ANALYSIS OF RESULTS OF QUASI-OPERATIONAL EXPERIMENTS

1. *Forecast of rainfall by tropical cyclone*

The forecast of rainfall by tropical cyclone has significant implications. Quasi-operational forecast experiments are carried out and the results scored in evaluating analysis with respect to all tropical cyclones that affected the south of China in 1993—1995. Work on the analysis of forecasts in 1993 is already in documentation①. Results only for 1994 and 1995 are studied.

Table 2 gives the TS statistics by 0—24 h, 12—36 h, and 24—48 h for all tropical cyclones in 1994 as predicted by ENPS and LAFS model of the National Meteorological Center. It is shown that except for the 48-h forecast in the 1 mm level, ENPS is advanta-

Table 2. Statistics of Treate-scores of rainfall predictions for typhoon cases affecting South China in 1994.

	ENPS						LAFS					
	LEV(mm)	TS	Po	Nh	Eh	B	LEV(mm)	TS	Po	Nh	Eh	B
24 h forecast	1	0.695	0.157	0.185	0.772	1.088	1	0.588	0.151	0.374	0.615	1.554
	10	0.478	0.296	0.362	0.727	1.170	10	0.254	0.586	0.572	0.650	1.569
	25	0.344	0.417	0.463	0.801	1.457	25	0.127	0.728	0.634	0.799	0.944
	50	0.218	0.582	0.665	0.887	1.314	50	0.048	0.911	0.833	0.888	0.448
	100	0.262	0.542	0.513	0.962	1.000	100	0.045	0.925	0.750	0.976	0.150
36 h forecast	1	0.697	0.127	0.216	0.740	1.199	1	0.661	0.034	0.329	0.673	1.720
	10	0.411	0.360	0.457	0.649	1.269	10	0.292	0.437	0.595	0.603	1.536
	25	0.253	0.543	0.573	0.705	1.432	25	0.175	0.592	0.654	0.703	2.760
	50	0.205	0.659	0.689	0.806	1.345	50	0.056	0.819	0.918	0.824	2.396
	100	0.127	0.792	0.833	0.948	0.698	100	0.034	0.900	0.929	0.943	0.367
48 h forecast	1	0.690	0.089	0.241	0.710	1.292	1	0.731	0.021	0.263	0.733	1.476
	10	0.382	0.388	0.471	0.610	1.369	10	0.380	0.334	0.486	0.599	1.518
	25	0.248	0.525	0.645	0.674	2.158	25	0.194	0.608	0.630	0.666	2.008
	50	0.188	0.625	0.706	0.831	1.236	50	0.049	0.858	0.866	0.745	1.145
	100	0.064	0.800	0.896	0.950	0.667	100	0.013	0.857	0.975	0.917	1.357

① Yan Jinghua and Xue Jishan, 1994. Verification and analysis of forecast by mesoscale numerical model of typhoon in 1993, In: Technical report on key project for the 8th five-year development program

geous over LAFS for all periods with all levels of rainfall (being high in TS but low in miss and false rates, exactly), particularly so in the 24 and 36 h periods at the levels of 25, 50, and 100 mm. The boundary condition is updated every 12 hours and provided by T42L9 model. Although it was altered to a longer period of 24 h from July 15, 1994 when T63 model with which ENPS was nested was officially in use, it is still much better in TS scores than LAFS for the same cases of tropical cyclone (table omitted).

The operational version is one that is nested with T63 model (in 12-h updating periods) and its quasi-operational forecasts are presented in Table 3 in terms of TS score statistics up till September, 1995 for all processes of tropical cyclones affecting the south of China. Similar high scores are with ENPS, especially, those for levels higher than 25 mm are better than the results for 1994 as shown in Table 2. It is conclusive that the superior forecast capability and stable performance of ENPS has given rise to much improved skills than the large scale LAFS rainfall predictive model of the National Meteorological Center for all corresponding levels of forecast.

Table 3. Same as Table. 2, but for typhoon cases before September 1995 with ENPS nested to T63.

	LEV(mm)	TS	Po	Nh	Eh	B
24 h forecast	1	0.616	0.154	0.265	0.728	1.543
	10	0.425	0.311	0.394	0.757	1.320
	25	0.475	0.304	0.299	0.860	1.128
	50	0.279	0.505	0.511	0.900	0.995
	100	0.253	0.472	0.563	0.957	0.905
36 h forecast	1	0.638	0.071	0.327	0.672	1.682
	10	0.464	0.212	0.460	0.698	1.680
	25	0.402	0.324	0.435	0.800	1.249
	50	0.331	0.471	0.344	0.888	0.993
	100	0.194	0.656	0.639	0.953	0.688
48 h forecast	1	0.720	0.007	0.277	0.729	1.423
	10	0.470	0.152	0.471	0.631	1.957
	25	0.313	0.444	0.523	0.728	1.337
	50	0.196	0.694	0.514	0.848	0.813
	100	0.064	0.840	0.813	0.944	0.600

A mean rather than particular skill of forecast is known from the table above. Time series are, therefore, examined in terms of the 50 mm-level TS scores for all individual forecasts of storm processes in 1994. In the case where T42 is nested, the mean rainfall score with ENPS (horizontal line) is always higher than LAFS for 24, 36, and 48 h periods. Though fluctuations of some degree appear in day-to-day TS values, null score cases in ENPS are fewer than in LAFS for all periods of forecast, judging from all events of validity. It further indicates that the model performs steadily with forecasts of rainfall over 50 mm, which is supported by the fact that there are much more events of valid forecasts of 50-mm rainfall (or, non-zero TS) than with LAFS. In contrast, there are fewer valid events in LAFS (only 3 times as compared with 10 times in LAFS) of forecast in, say, the 24-h period. It is concluded that LAFS gets low score for all periods while ENPS has high value.

Similar situations are found with cases after July 15, 1994 when ENPS is nested with T63 (figure omitted). Over this period, the score for LAFS (ENPS) is very low

(high) with much few (more) non-zero cases, i. e. the forecast of hard rain is effective and stable for the latter model.

Apart from the statistic values evaluated above, more real incidents of forecast are needed for further illustration. A severe tropical storm in 1994 (Russ) inflicted enormous floods by exceptional precipitation upon areas around Zhanjiang in the western part of Guangdong province and caused a loss of 5. 8 billion yuan (RMB). In retrospect, a hyetal region of 100 mm with a maximum of 200 mm near Zhanjiang was recorded at 1200 GMT 8 June, reviewing the rainfall observed and forecast at 1200 GMT on 8 and 9 June.

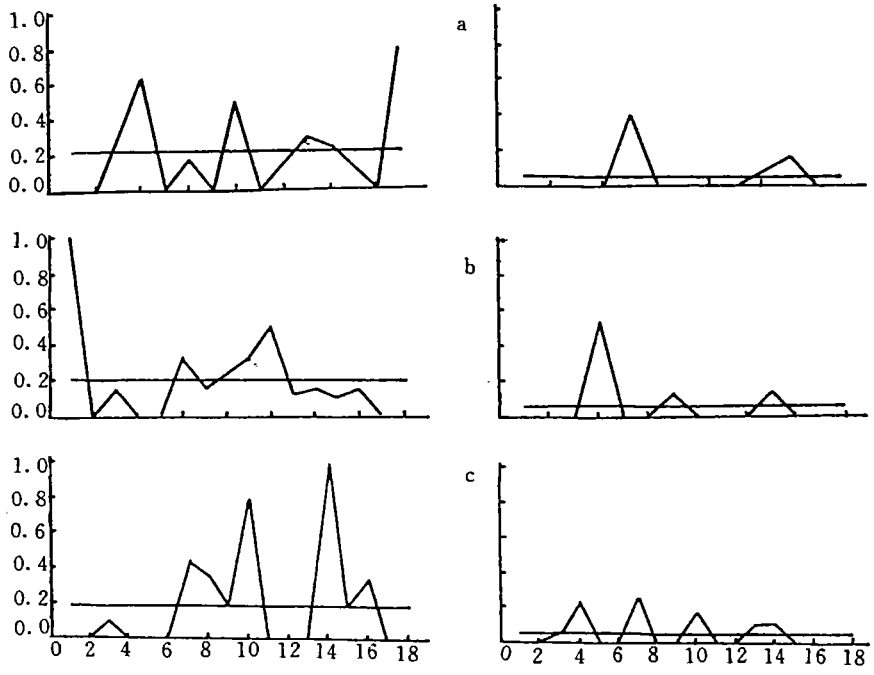

Fig. 3. Curves of TS for heavy rainfall (50 mm) forecasts for typhoon cases in 1994. Left pannels for ENPS & right pannels for LAFS, a, b & c stand for 24 h, 36 h & 48 h predictions respectively.

(The data are obtained from networked stations rather than intensive observation points or hydrological stations.) A rainfall of 25 mm is seen in most part of southern Guangdong. The forecast, on the other hand, turns to be close to the reality by displaying a hyetal region of 100 mm Zhanjiang through the north of Hainan (a little shrinked from the real situation) plus a center of 200 mm around Zhanjiang. Being close to the observations, the general distribution features heavier rainfall in the model for the northward central Guangdong than in the record. The observations at 1200 GMT 9 June of two rain zones of 100 mm and 50 mm (100 mm locally) respectively north of the Leizhou Peninsula and western Pearl River Delta, and a relatively lower rainfall between them, are well corresponded in the model, though more eastward location and less amount of rainfall are predicted concerning the intervening low-value and the eastern high-value zones. Satisfactory results are acquired by ENPS in the forecast of the storm process, which was just the system that had brought a heavy precipitation for two consecutive days and left

the area with devastating floods that was rare in history.

Another severe tropical storm Helen made landfall on the coast between Shenzhen and Huilai, Guangdong, in August 1995 and resulted in serious floods in the east of the province with a loss of 300 million yuan. The observed rainfall at 0000 GMT, 13 August 1995, around the time of landfall, and relevant 24-h forecast are given in Fig. 4. In the observation, a rainfall center of 200 mm around Huidong is associated with amount of 50-100 mm or beyond over all of eastern Guangdong; maxima in areas north of Hepu, Guangxi (above 50 mm) and western Pearl River Delta (above 25 mm), and relatively lower-value belts around Yangjiang, Dianbai and Xinyi and between Jiangmen and Zhaoqin, are alternatively distributed, showing a mesoscale pattern of maximal and minimal alternation in rainfall from the province of Guangxi to the east of Guangdong. The feature is well reproduced in the 24-h forecast (Fig. 4b), particularly with regard to the location of the maximum in Huidong, east of Guangdong, though the amount is 100 mm larger; a hyetal region of 200 mm is also predicted there in the 36-h range but with excessive amount in the Delta; rainfall of more than 100 mm is forecast Huidong through the western Pearl River Mouth with location of the center more to the west (figure omitted). In summary, the forecasts for periods of 24, 36, and 48 h can be relied on with considerable assurance, the 24-h results being the closest match.

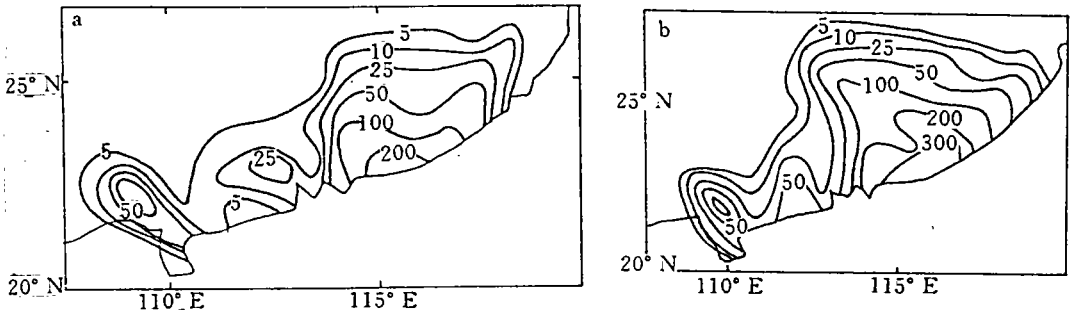

Fig. 4. 24 h precipitation at 0000 GMT 13 August 1995. a. observed; b. 24 h predicted.

2. *Forecast of track*

The forecast of track is the most interested aspect in a tropical cyclone. It is also an immediate factor that affects the rainfall forecast. As what is shown in the quasi-operational experiment, the average error in location forecast is well below the extreme limit for 200 and 400 km as far as the 24- and 48-h periods are concerned, in addition to capa*bility of handling complex motion of recurvature, suggesting skilled performance of* ENPS. A summary work is reported for the track forecast of tropical cyclone in 1993① and an account to such forecast for 1994 is also seen in a bulletin by the GRMC. Results concerning 1995 is elaborated here in this work.

According to the statistics of 14 forecasts of 4 tropical storms affecting the south of China, Helen, Irving, Lois, and Kent, by 31 August 1995 (Table 4), the error by ENPS is 116.6, 134.7, and 264.27 km, respectively for the periods of 24, 36, and 48 hours, which is lower than the mean error by centers in the United States, Japan, Australia and ECMWF, and far less than the limit requirement of motion prediction in the community

① Yan Jinghua and Xue Jishan, 1994. Verification and analysis of mesoscale NWP results of typhoon 1993.

(Chen, 1995).

Table 4. Statistics of track forecast errors for tropical cyclones in 1995 by the ENPS.

		Observation		24-h FC		24-h	36-h FC		36-h	48-h FC		48-h
		long.	lat.	long.	lat.	er. (km)	long.	lat.	er. (km)	long.	lat.	er.
Helen	00Z 11 Aug.	115.6	18.8	116.7	20.5	211.6						
	12Z 11 Aug.	115.1	20.8	114.2	20.7	94.6	115.3	21.8	23.4			
	00Z 12 Aug.	114.7	22.5	114.3	22.4	43.1	113.9	22.4	84.2	115	22.5	31.3
	12Z 12 Aug.	114.4	24.1	113.7	24.2	73.9	113.2	24	126.3	112.6	24.7	198.3
Irving	00Z 12 Aug.	111.7	19.5	112.2	18.9	81.6						
	12Z 19 Aug.	110.8	20.4	111.5	20.1	79.6	111.8	20.2	106.6			
Lois	00Z 28 Aug.	110.5	18.4	111.4	18.2	96.3						
	12Z 28 Aug.	108.8	19	110.7	20.2	170.1	110.6	20.2	261.8			
	00Z 29 Aug.	107.5	19	110	20.2	289.8	109.5	21.7	274.3	109.8	21.8	378.6
	12Z 29 Aug.	106.3	19.4	107.1	20.2	118.2	107.7	21.9	299.4	108.8	24.3	574.8
Kent	00Z 30 Aug.	122.2	20.1	121.9	19.9	37.7						
	12Z 30 Aug.	119.6	21.1	120	21.5	59.3	119.5	20.7	43.1			
	00Z 31 Aug.	116.8	22.3	116.5	23.1	89.3	117.9	22.4	115.9	117	21.9	41.8
	12Z 31 Aug.	113.5	23.3	114.3	24.9	186.9	114.6	23.7	122.3	116.9	23.9	360.8
Mean				0.44°	0.45°	116.6	0.69°	0.65°	134.7	1.15°	1.41°	264.3

Fig. 5a gives the observation and prediction (in a total of 4 successive 48-h periods) of Helen, a severe tropical storm in 1995 that posed significant influence on Guangdong. It is revealed that a sudden recurvature to the north in Helen's motion at 1200 GMT on

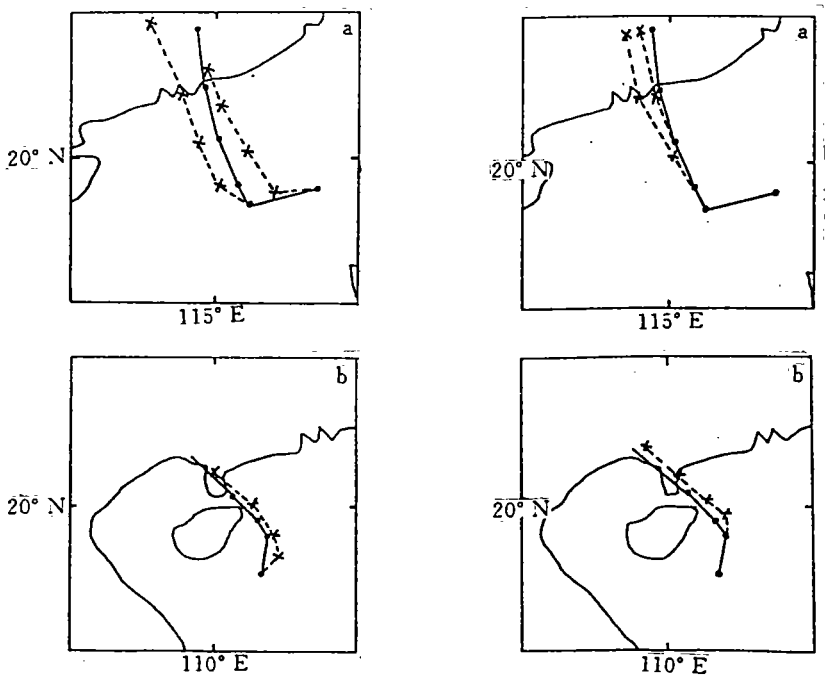

Fig. 5. Observed (solid) and predicted (dashed) tropical cyclone tracks.
a. Helen (first point at 0000 GMT 10 August 1995);
b. Irving (initial time 0000 GMT 18 August), interval 12 h.

10 August is missed by a subjective forecast by the Guangdong Meteorological Observatory (GMO) that it would land on the west of the province, while being foretold by ENPS 48 hours in advance in terms of the point of recurvature and landfall, and the time of landfall, in its output at intervals of 12 hours by error of less than 80 km and 3 h.

Fig. 5b plots the track observed and forecast for the tropical storm Irving, whose recurving and landing is predicted about 40 hours beforehand. It contrasts with the forecast by GMO in the morning of August 18 that the storm would move to north-northeast and make landfall near the Pearl River Mouth. It was just by ENPS that its sudden turn to the west was predicted in advance. Additionally, a similar motion in a most recent tropical cyclone Ryan was also outlined by ENPS while the subjective forecast by GMO at 0000 GMT 19 September 1995 failed to do so.

3. *Forecast of heavy rain in floods period*

It was widely reported that a heavy rain in June 1994 had evolved into a devastating floods rare in history for the south of China. A special attempt is done with ENPS to predict and assess the process that took place within what is called the "early floods season" there 11—18 June 1994①. One of the forecasts for 0000 GMT 17 June is selected for illustration of its performance.

Fig. 6 presents the observed rainfall and relevant field of forecast at 0000 GMT between 17 and 18 June. Being the last extensive process of precipitation in this sustaining wet period in June 1994, the raining belt did not travel out of the south of China until after 18 June. As shown in the figure, good consistence is found between the prediction and observation as well as the alignment of rain belts, mesoscale features and values of precipitation, with the best match of a 75-mm maximum in northern Guangdong but less strong reproduction of rainfall center for areas north of Zhanjiang.

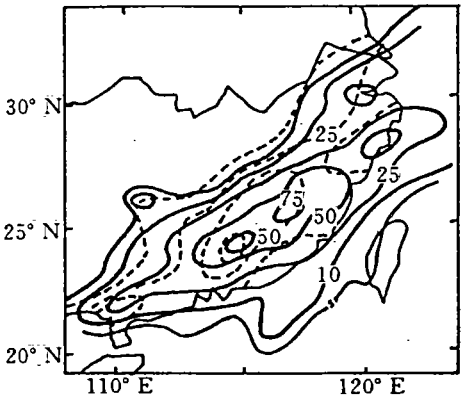

Fig. 6. Observed (dashed) and predicted (solid) 24 h precipitation at 0000 GMT 18 June 1994.

Fig. 7a, b, and c are 12-h forecast charts of the abovementioned fields of low-layer stream, temperature and vertical velocity, and Fig. 7d is the relevant observations of temperature, pressure, and wind. A vortex circulation is predicted at the lower (instead of middle and upper) layer in the northwest of Guangdong which acts as part of the whole frontal shear zone on the level. It is confirmed by corresponding low-level circulation observed, which is just in correspondence with the maximal zone of precipitation of more than 75 mm in the east and supporting the importance of the circulation in generation of the heavy rain. The prediction of temperature field, indicative of well-defined frontal and mesoscale signature, is impossibly shown in details in conventional observation and analyses. The prediction is also marked by a warm tongue over the Pearl River Delta to the east of the low layer vortex, which

① Wang Zaizhi and Yan Jinghua, 1994. Forecast and verification of sustaining heavy rains in southern China June 1994. In: Exchanges of the 9th Guangdong -Hong Kong Seminar on Important Weather, 114-126.

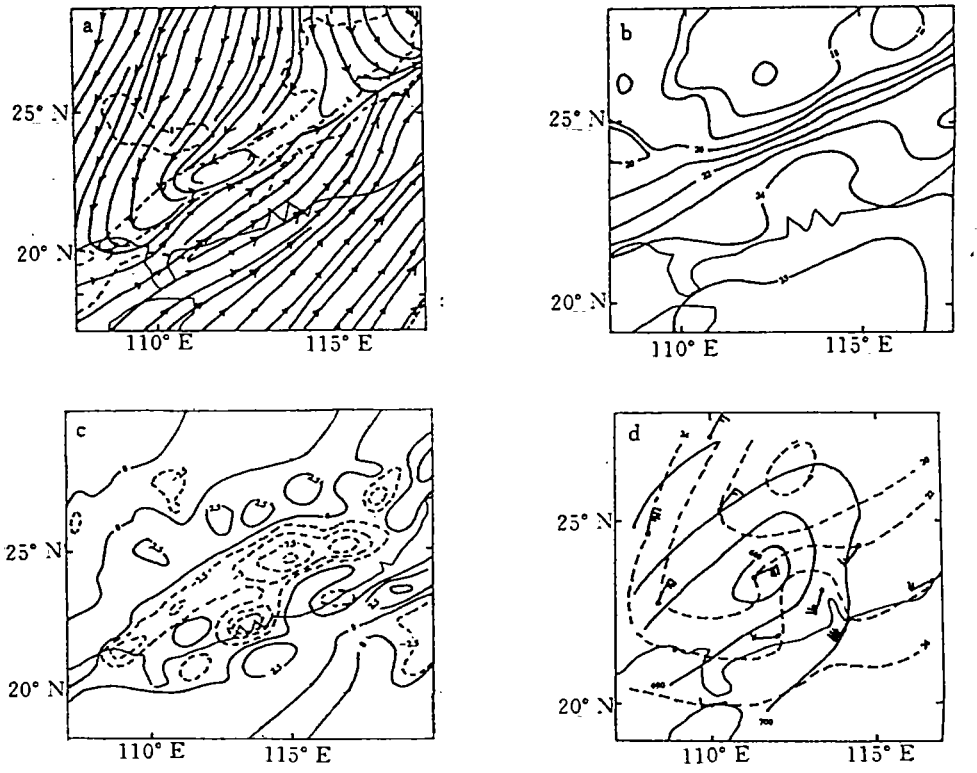

Fig. 7. 12 h predictions for stream line (a), temperature (b), vertical velocity (c, hPa/s) on 925 hPa valid at 1200 GMT 17 June 1994 and the corresponding observations (d).

is apparently caused by warm and moist air current. Along the northern edge of the tongue is exactly where the high-value region of precipitation sits for the north of Guangdong. Analysis of the observation also confirms of the existence of the warm tongue. An updraft is well depicted along strip-shaped frontal zone, together with a number of mesoscale uplifting cores therein, in the prediction of vertical velocity. They are considered in close relation with the high-value maxima of rainfall. The smaller downdraft, on the other hand, are also well reproduced behind the frontal zone.

To summarize, it is possible for ENPS to predict in an effective way the mesoscale features of fronts, temperature, pressure, wind and precipitation during the heavy rains in the so-call "early floods season".

4. *Conventional forecast*

Conventional weather forecasts are made twice daily with the quasi-operational ENPS, which suggests assuring capabilities for all weather phenomena in the south of China. Statistics of scores for a total of 36 experimental rainfall forecasts from 9 August to 5 September have shown equally high TS values (table omitted). Although the overall TS score is a little lower than individual cases, it is inherent in the methodology itself and does not imply less satisfactory outcome as compared with specific situation of tropical cyclone. For instance, the forecast efficiency for general weather processes (Eh) is normally higher than the process of the storm, which is convincing enough that ENPS is equally efficient for precipitation by conventional weather processes.

It is now clear that the performance of ENPS for all kinds of processes ensures reliable use in routine operation for issuance of high-resolution conventional forecasts of rainfall, surface winds, track of tropical cyclone, and meteorological elements in major towns of the country.

Ⅳ. CONCLUDING REMARKS

From the analyses in the sections above, the enhanced regional numerical prediction system is reliably useful for prediction of 0—48 h rainfall, tropical cyclone motion, heavy rains in the "early floods season", and conventional weather. Specifically, the score for rainfall prediction is higher than that by a predictive model of the National Meteorological Center and the mean error of track is lower than those by the centers in the United States and Japan in addition to capable handling of recurvative motion of a tropical cyclone. As the system is operation-friendly for both the running environment and efficiency, it is expected to have wide prospect for publicity in forefront applications. It was decided to put ENPS into official use from January 1996 in the Guangzhou Regional Meteorological Center.

REFERENCES

Anthes R A, Hsie Eirh-Yu, Kuo Ying-hua, 1987. Description of the PENN STATE/NCAR mesoscale model version 4 (MM4). NCAR TECHNICAL NOTE, NCAR/TN$_{xxx}$, 1—62.

Chen, Dehui, Yan Hong, 1995. Regional Modeling, Problems and Opportunities. PWPR Report Series No. 7. WMO/TD-No. 699, 1—8.

Chen Dehui, 1995. Latest progress in numerical prediction of tropical cyclones. *Meteor. Sci. & Tech.*, 3: 7—12 (in Chinese).

He Anguo, Wang Kangling, 1992. Numerical experiment with typhoons in the South China Sea of unusual track. *Journal of Tropical Meteorology*, 9: 133—141 (in Chinese).

Perkey D J, Kreitsberg C W, 1976. A time-dependent lateral boundary scheme for limited area primitive equation models. *Mon. Wea. Rev.*, 1976, 105: 744—755.

Xue Jishan, Wang Kangling, 1992. Objective analysis of wind and pressure fields in the tropics. *Scientia Atmospherica Sinica*, 16: 158—166 (in Chinese).

Yan Jinghua, Xue Jishan, 1995. Numerical analysis of diffusive difference between p-and σ-planes in mesoscale models. *Journal of Tropical Meteorology.*, 11: 354—364 (in Chinese).

Yan Hong, 1987. Research on nesting techniques with lateral boundary one-way influenced by limited-area predictive model. *Plateau Meteorology.*, 6 (supplementary): 192—197 (in Chinese).